The impact of right ventricular hemodynamics on the performance of a left ventricular assist device in a numerical simulation model

Author(s):
Thut, Titus L.Z.; Petrou, Anastasios; Meboldt, Mirko; Schmid Daners, Marianne; Wilhelm, Markus J.

Publication date:
2023-10-26

Permanent link:
https://doi.org/https://doi.org/10.3929/ethz-b-000610034

Originally published in:
Biomedical Engineering / Biomedizinische Technik 68(5), https://doi.org/10.1515/bmt-2020-0188

Titus L. Z. Thut, Anastasios Petrou, Mirko Meboldt, Marianne Schmid Daners and Markus J. Wilhelm*

The impact of right ventricular hemodynamics on the performance of a left ventricular assist device in a numerical simulation model

https://doi.org/10.1515/bmt-2020-0188
Received July 16, 2020; accepted April 3, 2023;
published online April 27, 2023

Abstract

Objectives: Left ventricular assist devices (LVADs) have been established as alternative to heart transplantation for patients with end-stage heart failure refractory to medical therapy. Right heart failure (RHF) after LVAD implantation is associated with inferior outcome. Its preoperative anticipation may influence the selection between a pure left ventricular and a biventricular device type and, thus, improve outcomes. Reliable algorithms to predict RHF are missing.
Methods: A numerical model was used for simulation of a cardiovascular circulation. The LVAD was placed as parallel circuit between left ventricle and aorta. In contrast to other studies, the dynamic hydraulic behavior of a pulsatile LVAD was replaced by that of a continuous LVAD. A variety of hemodynamic states was tested mimicking different right heart conditions. Adjustable parameters included heart rate (HR), pulmonary vascular resistance (PVR), tricuspid regurgitation (TR), right ventricular contractility (RVC) and pump speed. Outcome parameters comprised central venous pressure (CVP), mean pulmonary artery pressure (mPAP), cardiac output (CO) and occurrence of suction.
Results: Alteration of HR, PVR, TR, RVC and pump speed resulted in diverse effects on CO, CVP and mPAP, resulting in improvement, impairment or no change of the circulation, depending on the degree of alteration.
Conclusions: The numerical simulation model allows prediction of circulatory changes and LVAD behaviour following variation of hemodynamic parameters. Such a prediction may be of particular advantage to anticipate RHF after LVAD implantation. It may help preoperatively to choose the appropriate strategy of only left ventricular or both left and right ventricular support.

Keywords: advanced heart failure; hemodynamic parameters; left ventricular assist device; numerical simulation; right heart failure.

Introduction

Treatment with a left ventricular assist device (LVAD) has become a valuable option for patients with severely advanced heart failure refractory to medical therapy [1, 2]. It is applied as bridge to heart transplantation or as destination therapy in patients who are not suitable transplant candidates [3]. Overall survival of LVAD patients amounts to 83 % after one year, 73 % after two years, and 46 % after five years [4]. Predominant causes of death after LVAD implantation include stroke, multisystem organ failure, infection, and right heart failure (RHF) [4]. Death from RHF occurs primarily in the early months after LVAD implantation. Pre- or intraoperative identification of such patients is crucial to achieve favorable outcomes.

Right heart failure following LVAD implantation constitutes a flow imbalance between the left and right ventricle. The right ventricle is not able to pump enough blood through the pulmonary circulation for an adequate filling of the left ventricle. As a result, the right ventricle is overloaded, and the LVAD causes a progressive unloading of the left ventricle, ultimately resulting in the collapse of the left ventricle, a phenomenon known as suction, with subsequent circulatory failure [5–7].

Common reasons for RHF following LVAD implantation include preoperative impaired right ventricular function, elevated pulmonary artery pressure, dysrhythmia, perioperative hemorrhage and blood transfusion, infection, and sepsis [8, 9].

The prediction of RHF still remains a clinical challenge. A recent work of Bellavia et al. [10] presents a systematic

This study is part of the Zurich Heart project under the umbrella of University Medicine Zurich.

***Corresponding author: Markus J. Wilhelm**, Clinic for Cardiac Surgery, University Hospital Zurich, Rämistrasse 100, 8091 Zurich, Switzerland, Phone: +41 79 740 7307, Fax: +41 44 255 4467,
E-mail: markus.wilhelm@usz.ch
Titus L. Z. Thut, Clinic for Cardiac Surgery, University Hospital Zurich, Zurich, Switzerland
Anastasios Petrou, Mirko Meboldt and Marianne Schmid Daners, Product Development Group Zurich, Department for Mechanical and Process Engineering, ETH Zurich, Zurich, Switzerland

review and meta-analysis of predictors of RHF. The most important clinical predictors are the need for mechanical ventilation and continuous renal replacement therapy. The most important echocardiographic risk factors were shown to be moderate to severe right ventricular dysfunction and a larger right-to-left ventricular diameter ratio. Hemodynamically, the right ventricular stroke work index (RVSWI) and central venous pressure (CVP) had the strongest correlation with RHF development.

In RHF, an interplay of various hemodynamic parameters might cause a variety of reciprocal interactions between the pump, the left and right heart, and the circulation. To better understand these interactions, this study focused on characterizing the impact of various pump speed settings and right heart conditions on the pump performance and the circulation. For this purpose, a numerical simulation model of an LVAD-assisted human cardiovascular circulation was used.

Materials and methods

The numerical model of the cardiovascular circulation

All experiments were conducted using a numerical model described by Colacino et al. [11] and run on MATLAB/Simulink (The MathWorks, Inc., Natick, MA, USA). The model simulates the cardiovascular circulation of a human and is executable in real time. The performance of the numerical model has been presented earlier by Ochsner et al. [12]. It allows varying anatomical, physiological and pathological parameters during the simulation and consists of a mimicked adjustable systemic circulation imitating blood flow from the left heart to the periphery and back to the right heart, a pulmonary circulation imitating blood flow from the right heart to the lung and back to the left heart, and the heart activity as the mechanical drive. The model comprised the baroreflex, mimicking the pressure regulation in the systemic and pulmonary arterial trees that adapts the respective arterial resistance. A cardiac output autoregulation that adapts the unstressed volume of the systemic veins and the resistance of the systemic veins is adapted by a systemic venous resistance autoregulation. The implementation is described in detail in Ochsner et al. [12]. Figure 1 shows a simplified analog of the numerical cardiovascular model.

Four chambers simulate the heart. Two chambers represent the atria, which receive blood from the veins of the systemic circulation (i.e. right atrium) and from the pulmonary veins (i.e. left atrium), respectively, and deliver it to the right and left ventricles by contraction. The other two chambers constitute the right and left ventricles, which receive the blood from the atria and convey it to the great arteries (i.e. pulmonary artery and aorta) by contraction. The LVAD is placed as a parallel circuit between the left ventricle and the aorta. Cardiac contractions are simulated using a nonlinear, time-varying elastance model, with increased elastance during systole and decreased elastance during diastole. The heart valves are simulated as resistances, equipped with inductors to make them dynamic. This numerical model of a human cardiovascular circulation has been tested in numerous *in-vitro* studies [12–14].

Additionally, a ventricular suction emulation was incorporated into the numerical model, which simulates the pressure conditions due to the collapse of the left ventricle in case of insufficient blood supply to the left ventricle through the pulmonary circulation or excessive pump support. For the suction model, the simulated pump inlet pressure was used as the reference signal [15]. Left ventricular and pump inlet pressures match as long as no suction event occurs. When it comes to suction, the inflow cannula is blocked, which is modelled by a suction resistance, and the two pressures diverge. The suction resistance changes depending on the suction state and the pump inlet pressure downstream of this resistance is computed by subtracting the computed resistance multiplied by the pump flow from the left ventricular pressure.

Since continuous flow LVADs have mostly replaced pulsatile LVADs because they are associated with improved survival [16], we created a new simulation model by replacing the dynamic hydraulic behavior of a pulsatile LVAD, as used in the description of Colacino et al. [11] with that of a continuous flow LVAD, as the HeartWare HVAD (Medtronic, Minneapolis, MN, USA), based on the work by Granegger et al. [17]. The model relates the pressure (p) difference (H) between the inlet and outlet of the pump to the pump flow (Q). The algorithm incorporates the rotational speed (ω) of the pump, a static coefficient (a) related to the impeller speed, a static coefficient (b) related to the hydraulic resistance, and a constant value representing the fluid inertance (L), as described in the following equation: $H = a\omega^2 - bQ^2 - L\frac{dQ}{dt}$.

Experiments

In the experiments, we tested a broad variety of hemodynamic states, which mimic different right heart performances at different pump speeds. Adjustable parameters included heart rate (HR, bpm), pulmonary vascular resistance (PVR, dyn $\times$ s $\times$ cm^{-5}), tricuspid regurgitation (TR, degrees), and right ventricular contractility (RVC, % of normal), as well as LVAD speed (rpm). For further specification, RVC was defined using a time-varying elastance model, and the different degrees of TR were modelled by an increasing grade of resistance. Each of these parameters was altered separately in the four test series. Additionally, each test series was conducted at different LVAD pump speeds. Outcome parameters included suction occurrence, central venous pressure (CVP, mmHg), mean pulmonary arterial pressure (mPAP, mmHg), and cardiac output (CO, L/min).

The basic setup imitated a patient with a continuous flow LVAD implanted for left-sided heart failure, which was simulated by setting the left ventricular contractility to an ejection fraction of 30 % [11]. The tested pump speeds ranged from 2,400 to 3,200 rpm, according to the recommendations of the company and to clinical practice [18]. For the basic setup we used 2,400 rpm. The PVR in the basic setup was 150 dyn $\times$ s $\times$ cm^{-5}, which resulted in a physiologic mPAP of 18.01 mmHg [19]. At the basic setting, RVC was set to 100 %, HR to 70 bpm, and TR to degree 0 representing no TR.

In the four test series, one parameter of each of the basic settings was changed (Table 1). Each step of each series was additionally run at pump speeds from 2,400 to 3,200 rpm in increments of 160 rpm, or until suction occurred.

Results

Series I: Adjustment of HR

At an HR of 40 bpm, no suction occurred in the tested range. At 70 bpm suction occurred at a pump speed exceeding

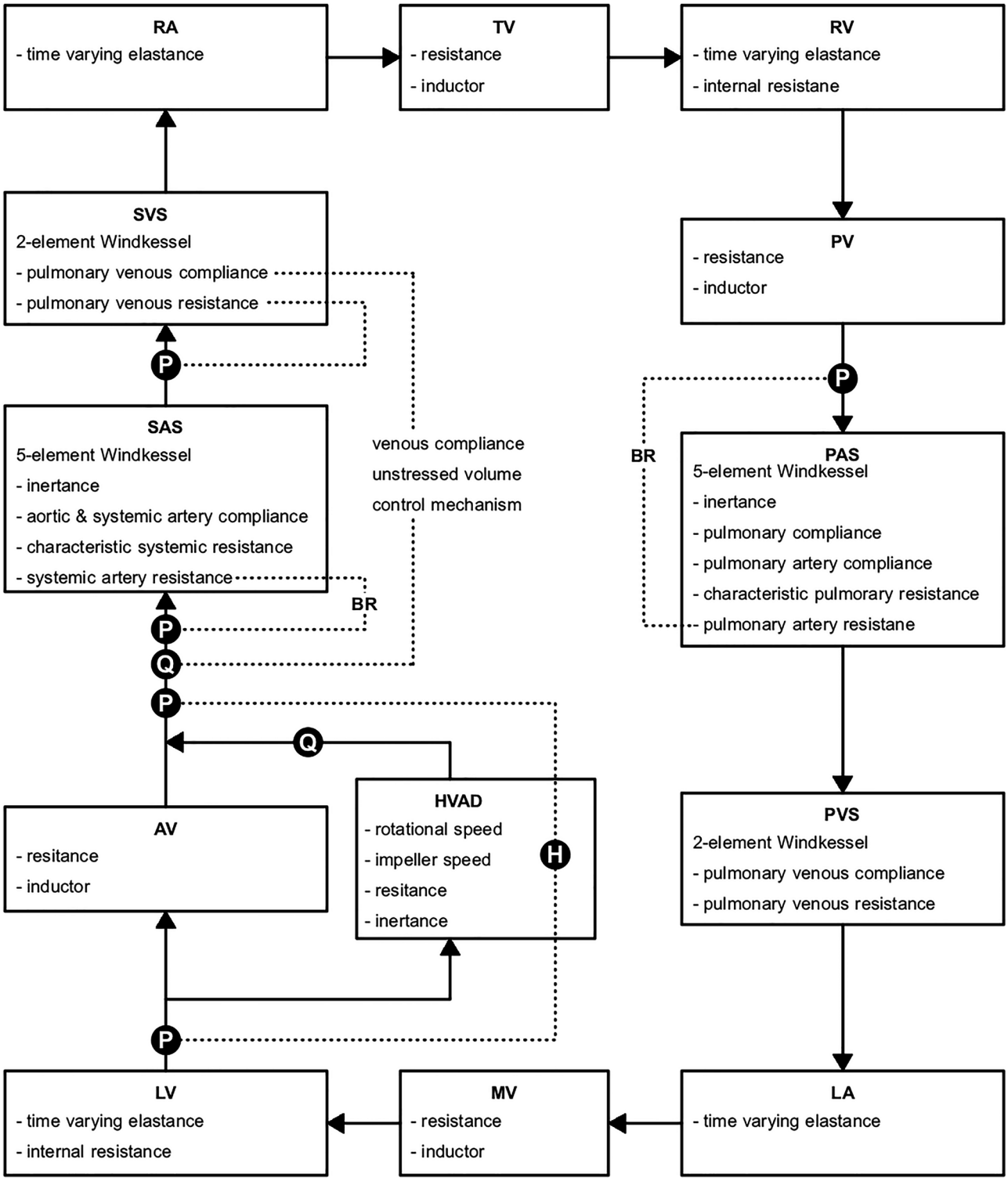

Figure 1: Analog of the numerical cardiovascular circulation model; a more precise description and validation can be found in Colacino et al. [11] and Granegger et al. [17]. (Arrows indicate flow and dashed lines indicate measurements; AV, aortic valve; BR, baroreflex; H, difference; LA, left atrium; LV, left ventricle; MV, mitral valve; P, pressure measurement; PAS, pulmonary arterial system; PV, pulmonary valve; PVS, pulmonary venous system; Q, flow; RA, right atrium; RV, right ventricle; SAS, systemic arterial system; SVS, systemic venous system; TV, tricuspid valve).

Table 1: Overview of all adjustable and outcome parameters (CO, cardiac output; CVP, central venous pressure; HR, heart rate; LVAD, left ventricular assist device; mPAP, mean pulmonary artery pressure; PVR, pulmonary vascular resistance; RVC, right ventricular contractility; TR, tricuspid regurgitation).

Series I	Series II	Series III	Series IV
HR, bpm	**PVR (dyn × s × cm^{-5})**	**TR (degree)**	**RVC, %**
40	150	0	100
70	300	1	80
100	450	2	60
130	600		40
160	750		
190	900		

Table 2A: Series I: Influence of HR on CVP, mPAP and CO at different pump speeds (CO, cardiac output; CVP, central venous pressure; HR, heart rate; mPAP, mean pulmonary artery pressure; PVR, pulmonary vascular resistance; RHF, right heart failure; RVC, right ventricular contractility; TR, tricuspid regurgitation).

Pump speed, rpm	2,400	2,560	2,720	2,880	3,040	3,200
Series I						
HR, bpm			CVP, mmHg			
40	7.30	7.55	7.78	8.01	8.22	8.26
70	7.05	7.28	7.51	7.72	7.93	Suction
100	6.98	7.15	7.37	7.57	7.75	Suction
130	7.06	7.21	7.43	7.63	7.81	Suction
160	7.13	7.29	7.52	7.72	7.90	Suction
190	7.29	7.46	7.68	7.88	8.08	Suction
			mPAP, mmHg			
40	17.89	16.77	15.88	15.01	14.30	14.21
70	18.02	17.05	16.18	15.52	14.72	Suction
100	17.98	17.26	16.42	15.77	15.18	Suction
130	17.90	17.27	16.43	15.76	15.19	Suction
160	17.90	17.23	16.37	15.72	15.13	Suction
190	17.84	17.13	16.30	15.66	14.92	Suction
			CO, L/min			
40	4.67	4.97	5.22	5.48	5.57	5.62
70	4.92	5.19	5.47	5.70	6.04	Suction
100	5.04	5.27	5.57	5.83	6.08	Suction
130	5.05	5.27	5.57	5.83	6.08	Suction
160	5.02	5.24	5.55	5.81	6.06	Suction
190	4.96	5.20	5.49	5.74	6.04	Suction

3,150 rpm (Table 2A). HRs at 100, 130, and 160 bpm caused suction when a pump speed of 3,090 rpm was exceeded. At 190 bpm, suction occurred above 3,150 rpm. At a given pump speed, an increase of HR did not change CVP, mPAP and CO (Figure 2a, example for a pump speed of 2,720 rpm). At all HRs, an increase of the pump speed caused a steady rise of the CVP and the CO and a decrease of the mPAP (Figure 2b, example for 100 bpm).

Series II: Adjustment of PVR

The higher the PVR, the earlier suction occurred. At a PVR of 150 dyn × s × cm^{-5} suction occurred beyond 3,150 rpm, at 900 dyn × s × cm^{-5} above 2,920 rpm Table 2B). An increase of the PVR steadily increased mPAP and slightly decreased CO at all pump speeds, but barely affected CVP (Figure 3a, example for a pump speed of 2,720 rpm). At a given PVR, an increase of pump speed led to a slight increase of CVP and CO as well as a decrease of mPAP (Figure 3b, example for a PVR of 600 dyn × s × cm^{-5}).

Series III: Adjustment of TR

Increasing TR let suction occur at lower pump speeds, at 3,150 rpm in TR 0, at 3,080 rpm in TR 1, and at 3,050 rpm in TR 2 (Table 2C). At all pump speeds, an increasing degree of TR led to a slight increase of CVP and a slight decrease of mPAP and CO (Figure 4a, example for a pump speed of 2,720 rpm). At all degrees of TR, increasing pump speed caused an increase of CVP and CO and a decrease of mPAP (Figure 4b, example for a TR degree 1).

Series IV: Adjustment of RVC

Reducing the RVC caused suction events at lower pump speeds (Table 2D). At 100 % RVC, suction occurred after exceeding a pump speed of 3,150 rpm and at 40 % RVC already exceeding 2,620 rpm. At all pump speeds, a decrease of RVC produced an increase of CVP and a decrease of mPAP and CO (Figure 5a, example for a pump speed of 2,560 rpm). At normal or only slighty reduced right ventricular contractility, an increase of pump speed caused a rise of cardiac output and central venous pressure as well as a reduction of mean pulmonary artery pressure. At more severely reduced right ventricular contractility, suction occurred more rapidly and at lower pump speeds than in the other test series (Figure 5b, for an example of 80 % RVC).

Discussion

The study presents a numerical model to simulate a circulation with an integrated continuous flow LVAD assisting the

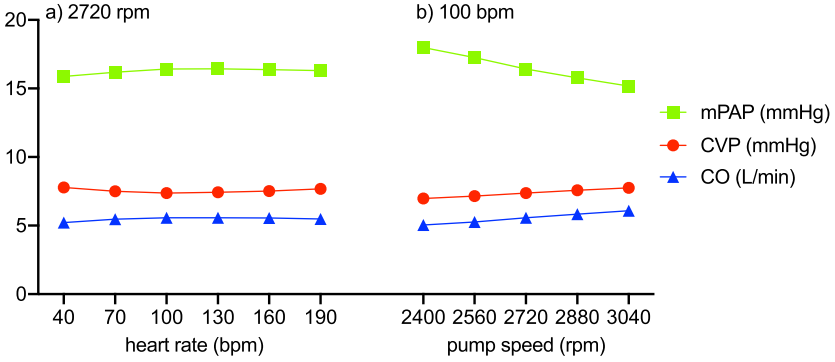

Figure 2: Series I: Influence of increasing HR on mPAP, CVP and CO at a constant pump speed of 2,720 rpm (Figure 2a), and influence of increasing pump speed on mPAP, CVP and CO at a constant HR of 100 bpm (Figure 2b) (bpm, beats per minute; CO, cardiac output; CVP, central venous pressure; HR, heart rate; mPAP, mean pulmonary artery pressure; rpm, rounds per minute).

Table 2B: Series II: Influence of PVR on CVP, mPAP and CO at different pump speeds (CO, cardiac output; CVP, central venous pressure; HR, heart rate; mPAP, mean pulmonary artery pressure; PVR, pulmonary vascular resistance; RHF, right heart failure; RVC, right ventricular contractility; TR, tricuspid regurgitation).

Pump speed, rpm	**2,400**	**2,560**	**2,720**	**2,880**	**3,040**	**3,200**
Series II						
PVR (dyn × s × cm^{-5})			CVP, mmHg			
150	7.05	7.28	7.51	7.72	7.93	Suction
300	7.04	7.27	7.50	7.71	7.93	Suction
450	7.02	7.26	7.49	7.69	Suction	Suction
600	7.01	7.25	7.48	7.68	Suction	Suction
750	7.01	7.25	7.47	7.68	Suction	Suction
900	7.04	7.28	7.50	7.75	Suction	Suction
			mPAP, mmHg			
150	18.02	17.05	16.18	15.52	14.72	Suction
300	21.69	20.83	20.09	19.54	18.77	Suction
450	25.88	25.13	24.54	24.10	Suction	Suction
600	30.01	29.38	28.92	28.57	Suction	Suction
750	34.08	33.57	33.22	32.96	Suction	Suction
900	38.14	37.73	37.47	37.16	Suction	Suction
			CO, L/min			
150	4.92	5.19	5.47	5.70	6.04	Suction
300	4.87	5.15	5.42	5.65	5.98	Suction
450	4.82	5.10	5.37	5.59	Suction	Suction
600	4.77	5.06	5.31	5.53	Suction	Suction
750	4.71	5.00	5.25	5.46	Suction	Suction
900	4.64	4.93	5.16	5.38	Suction	Suction

Table 2C: Series III: Influence of TR on CVP, mPAP and CO at different pump speeds (CO, cardiac output; CVP, central venous pressure; HR, heart rate; mPAP, mean pulmonary artery pressure; PVR, pulmonary vascular resistance; RHF, right heart failure; RVC, right ventricular contractility; TR, tricuspid regurgitation).

Pump speed, rpm	**2,400**	**2,560**	**2,720**	**2,880**	**3,040**	**3,200**
Series III						
TR (degree)			CVP, mmHg			
TR 0	7.05	7.28	7.51	7.72	7.93	Suction
TR 1	7.58	7.81	8.01	8.19	8.36	Suction
TR 2	7.73	7.95	8.15	8.33	8.48	Suction
			mPAP, mmHg			
TR 0	18.02	17.05	16.18	15.52	14.72	Suction
TR 1	17.07	16.13	15.41	14.81	14.24	Suction
TR 2	16.79	15.88	15.19	14.57	14.11	Suction
			CO, L/min			
TR 0	4.92	5.19	5.47	5.70	6.04	Suction
TR 1	4.68	4.99	5.25	5.48	5.65	Suction
TR 2	4.63	4.93	5.19	5.42	5.56	Suction

heart during left ventricular failure. It allows a prediction of circulatory changes and pump performance following variations of hemodynamic parameters. Here, parameters associated with right ventricular function were in the focus of the simulation.

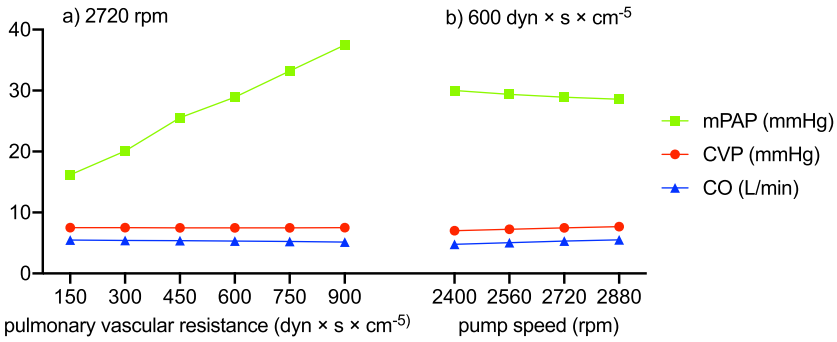

Figure 3: Series II: Influence of increasing PVR on mPAP, CVP and CO at a constant pump speed of 2,720 rpm (Figure 3a), and influence of increasing pump speed on mPAP, CVP and CO at a constant PVR of 600 dyn × sec × cm^{-5} (Figure 3b) (CO, cardiac output; CVP, central venous pressure; mPAP, mean pulmonary artery pressure; PVR, pulmonary vascular resistance; rpm, rounds per minute).

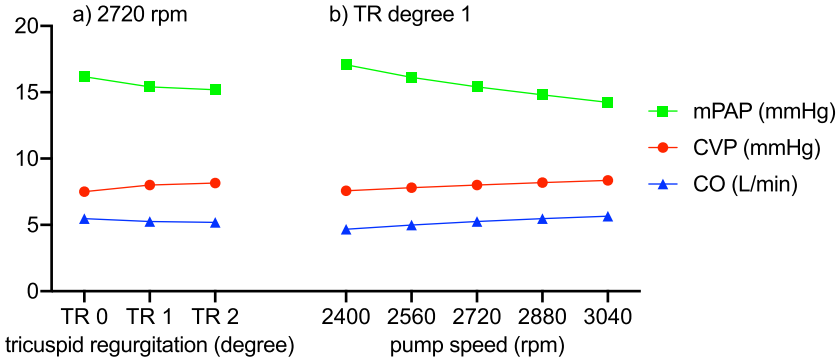

Figure 4: Series III: Influence of increasing TR on mPAP, CVP and CO at a constant pump speed of 2,720 rpm (Figure 4a), and influence of increasing pump speed on mPAP, CVP and CO at a constant TR of degree 1 (Figure 4b) (CO, cardiac output; CVP, central venous pressure; mPAP, mean pulmonary artery pressure; TR, tricuspid regurgitation; rpm, rounds per minute).

Table 2D: Series IV: Influence of RVC on CVP, mPAP and CO at different pump speeds (CO, cardiac output; CVP, central venous pressure; HR, heart rate; mPAP, mean pulmonary artery pressure; PVR, pulmonary vascular resistance; RHF, right heart failure; RVC, right ventricular contractility; TR, tricuspid regurgitation).

Pump speed, rpm	**2,400**	**2,560**	**2,720**	**2,880**	**3,040**	**3,200**
Series IV						
RVC, %			CVP, mmHg			
100	7.05	7.28	7.51	7.72	7.93	Suction
80	7.06	7.29	7.52	7.73	7.95	Suction
60	7.17	7.40	7.61	7.81	Suction	Suction
40	9.48	9.60	Suction	Suction	Suction	Suction
			mPAP, mmHg			
100	18.02	17.05	16.18	15.52	14.72	Suction
80	17.78	16.81	15.97	15.33	14.49	Suction
60	17.13	16.19	15.44	14.81	Suction	Suction
40	12.88	12.37	Suction	Suction	Suction	Suction
			CO, L/min			
100	4.92	5.19	5.47	5.70	6.04	Suction
80	4.87	5.15	5.42	5.65	5.95	Suction
60	4.69	5.01	5.27	5.50	Suction	Suction
40	3.79	4.03	Suction	Suction	Suction	Suction

The measurements in Series I with varying HRs and otherwise normal hemodynamic parameters simulated a typical performance of an LVAD. An increase of the pump speed led to more flow and a rising CO, which caused a decrease of pressure in the lung circulation (mPAP). Right ventricular preload, as measured by the CVP, increased, since more blood volume was pumped from the left to the right side.

HRs of up to 190 bpm did not disturb the pump performance and the resulting circulatory support, as long as the pump speed was not set to the maximum of 3,200 rpm, which is clinically irrelevant. Ventricular tachycardia with HRs above 130 bpm are a well-known phenomenon in heart failure [20]. As a consequence, acute RHF may develop with subsequent insufficient blood supply to the left ventricle, which causes a potential hazardous reduction of CO through the LVAD. The simulation shows that, despite the tachycardia, a regular pump performance and sufficient circulation are maintained, at least as long as the other hemodynamic parameters which were simulated, such as PVR, TR and RVC, are kept within a physiological range.

Elevated PVR is a common condition in patients with left heart failure [21]. Test Series II shows that, with rising PVR, the CO is gradually reduced. This corresponds to the circumstances in a human circulation and can be explained by the reduction of blood flow through the lungs at elevated levels of PVR which, in turn, leads to a decrease of blood supply to the LVAD and a consecutive reduction of CO. Augmentation of the pump speed can restore the CO to a certain extent until, ultimately, left ventricular suction occurs. As a result, mPAP is reduced, but not as much as in Test Series I when PVR was kept normal.

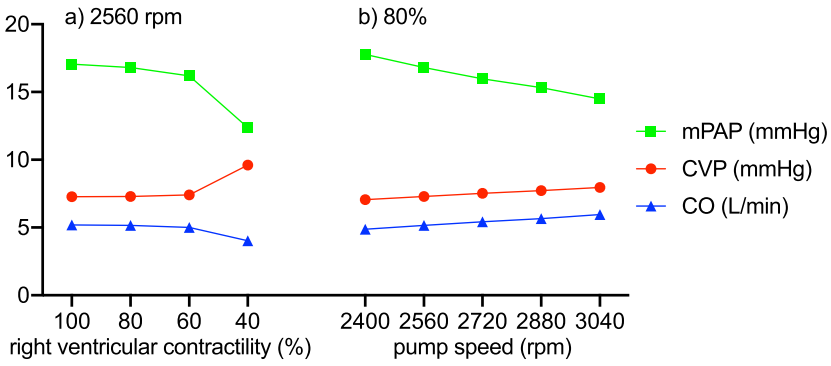

Figure 5: Series IV: Influence of decreasing RVC on mPAP, CVP and CO at a constant pump speed of 2,560 rpm (Figure 5a), and influence of increasing pump speed on mPAP, CVP and CO at a constant RVC of 80 % (Figure 5b) (CO, cardiac output; CVP, central venous pressure; mPAP, mean pulmonary artery pressure; RVC, right ventricular contractility; rpm, rounds per minute).

TR frequently occurs in heart failure due to a dilatation of the right ventricle with a subsequent widening of the tricuspid ring [22]. In TR, the blood flow is not fully directed forward into the pulmonary circulation, but partly backwards into the right atrium. The test Series III simulated this hemodynamic consequence. With increasing TR, the CVP increases due to a larger amount of blood volume in the right atrium, while mPAP and CO decrease, since less blood is available for antegrade flow through the pulmonary circulation into the left ventricle and, consequently, for the LVAD to pump. Augmentation of the pump speed increases the CO, which further decreases the mPAP and elevates the CVP because more blood is pumped back to the right ventricle. However, excessive pump speeds may result in suction due to the limited left ventricular preload.

RVC constitutes the most decisive parameter for a proper functioning of an LVAD-equipped circulation [23]. Impairment of RVC causes a reduction of blood flow through the lungs and to the left ventricle such that the LVAD is not able to pump enough blood for maintaining a sufficient circulation. This is demonstrated in Test Series IV. The decrease of RVC leads to an increase of CVP since the ability of the right ventricle to forward the blood to the lungs is reduced. This causes a drop of the mPAP and a decrease of left ventricular volume resulting in a decline of LVAD capacity and CO. Increase of pump speed can counteract the condition to a certain extent. But particularly in severely reduced RVC, the elevation of pump speed leads to suction episodes and a compromise of the circulation.

The numerical simulation model presented here provides us with the unique possibility to examine the impact of isolated hemodynamic parameters on a circulation with a continuous flow LVAD. The simulation of suction events was implemented because, in clinical reality, suction may be associated with potentially life threatening adverse events such as ventricular arrhythmias or tachycardia, damage to the heart muscle, or thrombus formation in the pump [24, 25].

The most unpredictable parameter after LVAD implantation is the performance of the right ventricle [8]. If implantation of a right ventricular assist device (RVAD) is needed due to right ventricular failure after LVAD implantation, mortality increases considerably [4]. Various scores which were developed to predict the risk of RHF after LVAD placement did not prove to be reliable in clinical practice [10]. Unfortunately, as Raina and Patarroyo-Aponte outlined in their review, one of the problems with risk prediction scores is that they have not been validated well outside of their derivation cohorts, and their predictive value in validation cohorts is likely lower than in the derivation cohorts [26]. Recently, echocardiographic parameters such as right ventricular free wall longitudinal strain and RVSWI have been suggested as good predictors for right heart failure [27]. However, both indices may be used only in addition to other parameters predictive for RHF.

Assessment of right ventricular contractility appears to be of particular importance for a prediction of RHF. If the simulation should reveal an increased risk for RHF after LVAD placement, the operative strategy might already preoperatively be changed from a sole LVAD to an LVAD with a temporary RVAD or a durable biventricular assist device [28].

Furthermore, the simulation model may help to predict the optimal pump speed after LVAD implantation. It is a balancing act to set the pump speed such that a sufficient CO is generated by the LVAD and, at the same time, the right ventricle does not fail due to volume overload. Thus, prediction of the hemodynamic situation after LVAD implantation by simulating different pump speeds and integrating the patient's preoperative hemodynamic parameters could provide guidance for setting the suitable pump speed for optimal cardiovascular support.

One limitation of the numerical model presented here is the fact that it is not validated and, thus, may not be able to serve as a tool to assess the risk for RHF after LVAD implantation in its present form. Also, adaptation of the volume status to simulate venous overload frequently associated with right heart failure was not incorporated in the model. Another limitation of the study is that the numerical simulation model cannot consider the multiple parameters which influence the hemodynamics in a live circulation with an integrated LVAD. Various aspects, such as the interventricular septum, the pericardium, recirculation zones or wave propagations, or even more complex biochemical processes which exert an impact on hemodynamics, are demanding to simulate and are not incorporated in this model. Yet, adding such features to the model would bring the simulation even closer to reality. The effect of the integrated baroreflex mechanism, however, may be treated with caution. Next steps will be to adapt the simulation algorithm to animal models before it may be applied in the clinic.

In summary, based on individual simulations of patient-specific parameters, the numerical model presents an instrument to predict hemodynamic alterations after LVAD implantation. Such a prediction may be of particular advantage to anticipate RHF which constitutes a frequent problem after LVAD implantation. The simulation may help to make the appropriate choice between only left ventricular or both left and right ventricular support, and it may assist in the selection of the appropriate pump speed of the LVAD.

Acknowledgments: This work is part of the Zurich Heart project under the umbrella of University Medicine Zurich. We thank Mrs. Brigitte Rohrbach, the former secretary of the

Institute for Dynamic Systems and Control at the ETH Zurich, Switzerland, for revision of the English language.
Research funding: None declared.
Author contributions: All authors have accepted responsibility for the entire content of this manuscript and approved its submission.
Competing interests: Authors state no conflict of interest.
Informed consent: Not applicable.
Ethical approval: Not applicable.

References

1. Feldman D, Pamboukian SV, Teuteberg JJ, Birks E, Lietz K, Moore SA, et al. The 2013 international society for heart and lung transplantation guidelines for mechanical circulatory support: executive summary. J Heart Lung Transplant 2013;32:157–87.
2. Ponikowski P, Voors AA, Anker SD, Bueno H, Cleland JGF, Coats AJS, et al. 2016 ESC Guidelines for the diagnosis and treatment of acute and chronic heart failure: the task Force for the diagnosis and treatment of acute and chronic heart failure of the European Society of Cardiology (ESC). Developed with the special contribution of the heart failure association (HFA) of the ESC. Eur J Heart Fail 2016;18:891–975.
3. Wilhelm MJ, Ruschitzka F, Falk V. Destination therapy – time for a paradigm change in heart failure therapy. Swiss Med Wkly 2013;143: w13729.
4. Kormos RL, Cowger J, Pagani FD, Teuteberg JJ, Goldstein DJ, Jacobs JP, et al. The society of thoracic surgeons intermacs database annual report: evolving indications, outcomes, and scientific partnerships. J Heart Lung Transplant 2019;38:114–26.
5. Reesink K, Dekker A, Van der Nagel T, Beghi C, Leonardi F, Botti P, et al. Suction due to left ventricular assist: implications for device control and management. Artif Organs 2007;31:542–9.
6. Vollkron M, Schima H, Huber L, Wieselthaler G. Interaction of the cardiovascular system with an implanted rotary assist device: simulation study with a refined computer model. Artif Organs 2002;26:349–59.
7. AlOmari AHH, Savkin AV, Stevens M, Mason DG, Timms DL, Salamonsen RF, et al. Developments in control systems for rotary left ventricular assist devices for heart failure patients: a review. Physiol Meas 2013;34:R1–27.
8. Lampert BC, Teuteberg JJ. Right ventricular failure after left ventricular assist devices. J Heart Lung Transplant 2015;34:1123–30.
9. Loghmanpour NA, Kormos RL, Kanwar MK, Teuteberg JJ, Murali S, Antaki JF. A Bayesian model to predict right ventricular failure following left ventricular assist device therapy. JACC Heart Fail 2016;4:711–21.
10. Bellavia D, Iacovoni A, Scardulla C, Moja L, Pilato M, Kushwaha SS, et al. Prediction of right ventricular failure after ventricular assist device implant: systematic review and meta-analysis of observational studies. Eur J Heart Fail 2017;19:926–46.
11. Colacino FM, Moscato F, Piedimonte F, Arabia M, Danieli GA. Left ventricle load impedance control by apical VAD can help heart recovery and patient perfusion: a numerical study. ASAIO J 2007;53:263–77.
12. Ochsner G, Amacher R, Amstutz A, Plass A, Schmid Daners M, Tevaearai H, et al. A novel interface for hybrid mock circulations to evaluate ventricular assist devices. IEEE Trans Biomed Eng 2013;60:507–16.
13. Colacino FM, Arabia M, Danieli GA, Moscato F, Nicosia S, Piedimonte F, et al. Hybrid test bench for evaluation of any device related to mechanical cardiac assistance. Int J Artif Organs 2005;28:817–26.
14. Colacino FM, Arabia M, Moscato F, Danieli GA. Modeling, analysis, and validation of a pneumatically driven left ventricle for use in mock circulatory systems. Med Eng Phys 2007;29:829–39.
15. Ochsner G, Amacher R, Schmid Daners M. Emulation of ventricular suction in a hybrid mock circulation. In: 2013 european control conference (ECC). IEEE; 2013:3108–12 pp.
16. Slaughter MS, Rogers JG, Milano CA, Russell SD, Conte JV, Feldman D, et al. Advanced heart failure treated with continuous-flow left ventricular assist device. N Engl J Med 2009;361:2241–51.
17. Granegger M, Moscato F, Casas F, Wieselthaler G, Schima H. Development of a pump flow estimator for rotary blood pumps to enhance monitoring of ventricular function. Artif Organs 2012;36: 691–9.
18. HeartWare. Heartware® ventricular assist system – instructions for use [Internet]. Available from: http://www.heartware.com/sites/default/files/uploads/docs/ifu00001_rev_15.pdf [Accessed 1 Oct 2019].
19. Schmidt RF, Lang F, Thews G, editors. Physiologie des Menschen. Berlin, Heidelberg: Springer; 2005.
20. Zhang D, Tu H, Wadman MC, Li YL. Substrates and potential therapeutics of ventricular arrhythmias in heart failure. Eur J Pharmacol 2018;833:349–56.
21. Fabregat-Andrés Ó, Estornell-Erill J, Ridocci-Soriano F, García-González P, Bochard-Villanueva B, Cubillos-Arango A, et al. Prognostic value of pulmonary vascular resistance estimated by cardiac magnetic resonance in patients with chronic heart failure. Eur Heart J Cardiovasc Imaging 2014;15:1391–9.
22. Dreyfus GD, Martin RP, Chan KMJ, Dulguerov F, Alexandrescu C. Functional tricuspid regurgitation: a need to revise our understanding. J Am Coll Cardiol 2015;65:2331–6.
23. Kormos RL, Teuteberg JJ, Pagani FD, Russell SD, John R, Miller LW, et al. Right ventricular failure in patients with the HeartMate II continuous-flow left ventricular assist device: incidence, risk factors, and effect on outcomes. J Thorac Cardiovasc Surg 2010;139:1316–24.
24. Vollkron M, Voitl P, Ta J, Wieselthaler G, Schima H. Suction events during left ventricular support and ventricular arrhythmias. J Heart Lung Transplant 2007;26:819–25.
25. Wang Y, Simaan MA. A suction detection system for rotary blood pumps based on the Lagrangian support vector machine algorithm. IEEE J Biomed Health Inform 2013;17:654–63.
26. Raina A, Patarroyo-Aponte M. Prevention and treatment of right ventricular failure during left ventricular assist device therapy. Crit Care Clin 2018;34:439–52.
27. Gumus F, Durdu MS, Cakici M, Kurklu TST, Inan MB, Dincer I, et al. Right ventricular free wall longitudinal strain and stroke work index for predicting right heart failure after left ventricular assist device therapy. Interact Cardiovasc Thorac Surg 2019;28:674–82.
28. Dandel M, Krabatsch T, Falk V. Left ventricular vs. biventricular mechanical support: decision making and strategies for avoidance of right heart failure after left ventricular assist device implantation. Int J Cardiol 2015;198:241–50.

Supplementary Material: This article contains supplementary material (https://doi.org/10.1515/bmt-2020-0188).